

THE INFLUENCE OF WATER VAPOR ADDITION ON
HYDROGEN-OXYGEN DETONATIONS

B. F. Kerkam
E. K. Dabora

ORA Project 06996

under contract with

U. S. Army Research Office (Durham)
Contract No. DA-31-124-ARO-D-299
Durham, North Carolina

Aircraft Propulsion Laboratory
Department of Aeronautical and Astronautical Engineering
The University of Michigan
Ann Arbor, Michigan

April 1965

ABSTRACT

The minimum detonation Mach number, below which detonative combustion is not possible, can be predicted by Belles' explosion limit criterion for H_2-O_2 mixtures. The criterion predicts also that the addition of water vapor increases this minimum Mach number. The experiments which are described here and which are based on the technique of slowing down an established Chapman-Jouguet detonation wave by exposing one of its sides to a compressible boundary verify this prediction. It is found that the addition of 2% water vapor to a stoichiometric H_2-O_2 mixture increases the minimum detonation Mach number by 3% as predicted by theory. It is also found that the same amount of water vapor decreases the reaction length by approximately 50% and that the addition of 1% of water vapor to 50% hydrogen-50% oxygen mixtures reduces the reaction length by approximately 30%. The experimental work of Kistaikowsky and Kydd is found to support the latter findings.

ACKNOWLEDGMENTS

The work described in this report was initially started under Grant No. DA-ARO(D)-31-124-G-345 by the U. S. Army Research Office (Durham). Its completion was made possible, however, by contract No. DA-31-124-ARO-D-299 from the same agency. The authors are therefore very grateful to ARO for its financial assistance.

The authors wish to thank Professor J. A. Nicholls, Project Supervisor, for his guidance and advice during all phases of this work and to those among the staff of the Aircraft Propulsion Laboratory who assisted in many ways during this project.

TABLE OF CONTENTS

	Page
ABSTRACT	iii
ACKNOWLEDGMENTS	v
LIST OF FIGURES	ix
NOMENCLATURE	xi
I. INTRODUCTION	1
II. EXPERIMENTAL ARRANGEMENTS AND PROCEDURE	5
III. EXPERIMENTAL RESULTS	11
IV. DISCUSSION	17
V. CONCLUSIONS	20
REFERENCES	21
APPENDIX I. Calibration Curves for DewProbe/Thermistor Dewpoint Measurement System	31

LIST OF FIGURES

	Page
Figure 1. Maximum Allowable Mach Number Decrement as a Function of Water Vapor Content	22
Figure 2. Model for the Interaction of a Detonation with a Compressible Inert Boundary	23
Figure 3. Schematic of Mixing and Charging System	24
Figure 4. Circuit Diagram for DewProbe Cavity Temperature Measurement	25
Figure 5. Calibration Curve for Use in Determining Water Vapor Content of Explosive Mixture from Thermistor Current Flow	26
Figure 6. Experimental Mach Number Decrement Due to the Compressible Boundary as a Function of Channel Width. 50% H ₂ + 50% O ₂ Mixture	27
Figure 7. Detonation Velocity of 50% H ₂ + 50% O ₂ and 66 2/3% H ₂ + 33 1/3% O ₂ Mixtures as a Function of Water Vapor Content	28
Figure 8. Experimental Mach Number Decrement Due to the Compressible Boundary as a Function of Channel Width. 66 2/3% H ₂ + 33 1/3% O ₂ Mixture	29
Figure 9. Density Changes in a Hydrogen-Oxygen Detonation as a Function of Time. Data from Kistiakowsky and Kydd	30
Figure a - Thermistor Calibration Temperature vs. Current Through Thermistor	32
Figure b - Dewpoint vs. DewProbe Cavity Temperature	33
Figure c - Volumetric Concentration of H ₂ O Vapor vs. Mixture Dewpoint	34

NOMENCLATURE

a	velocity of sound
b	explosive channel width, inches
d	tube diameter
E	activation energy for chemical reaction
f	mole fraction
$k_1, k_2, \text{ etc.}$	reaction rate constants for reactions I, II, etc.
M	Mach number
p	pressure
R	universal gas constant
T	temperature
V	detonation velocity
(X)	third body concentration
\bar{x}	reaction length
γ	ratio of specific heats
δ^*	displacement thickness
ρ	density

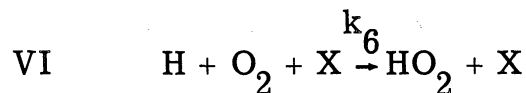
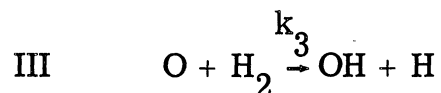
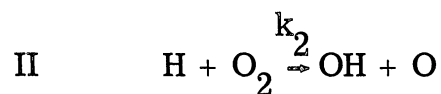
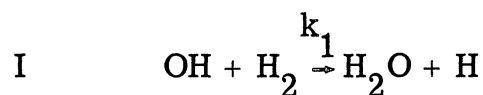
Subscripts

a	ambient
cr	critical
D	detonation
e	explosive
ex	after expansion
i	inert
th	theoretical
w	water
0	initial conditions

I. INTRODUCTION

The purpose of this research is to investigate the effect of water vapor on the quenching of detonations in hydrogen-oxygen mixtures which are between the lean and rich limits of detonation. The explosion limit criterion proposed by Belles⁽¹⁾ for finding the composition limits of detonability has been shown by Dabora⁽²⁾ to be an accurate description of the limits of detonability for hydrogen-oxygen mixtures. However, Belles' criterion essentially utilizes the "second explosion limit" chemical-kinetic equations while pressure and temperature conditions in the induction zone of typical hydrogen-oxygen detonation are far from the second limit conditions. It is not, therefore, clear that the chemical-kinetic equations which describe the second explosion limit can be applied in general to the problem of describing the conditions at which detonation waves will quench. This research is a continuation of Dabora's work, intended to further explore the correctness of applying Belles' explosion limit criterion to the detonation quenching problem.

Belles' chemical-kinetic formulation of the detonation quenching problem utilizes the following reactions:*



*Numbered according to the convention given by Lewis and von Elbe⁽³⁾.

It follows from the steady state approximation that the net rate of production of active species (O, OH, H) in the induction zone will fall to zero when:

$$2k_2 = k_6(X) \quad (1)$$

If this condition is obtained, it is expected that an existing detonation will cease to propagate as a detonation (i. e. , quench), or that a detonation cannot be initiated. Here, X is the effective third body concentration defined by the empirical relation given by Lewis and von Elbe⁽³⁾:

$$f_x \equiv f_{H_2} + .35f_{O_2} + 14.3f_{H_2O} + .43f_{N_2} + .36f_{He} + .20f_{Ar} + 1.47f_{CO_2} \quad (2)$$

Equation (2) points out the high efficiency of water vapor as a third body in the chain-breaking reaction, reaction VI. Using the appropriate reaction rates for reactions I, II, III, and VI, and using shock wave relations to determine pressure and temperature in the induction zone allowed Belles to develop a relation which can be solved for the critical, or minimum allowable Mach number of detonation. The relation given by Belles is:

$$\log_{10} \frac{3.11}{f_x} = \frac{3710 \alpha^2 \beta^2 M_{cr}^2}{T_0 \left(\frac{M_{cr}^2}{\beta} - 1 \right) \left(\beta M_{cr}^2 + \frac{1}{\gamma} \right)} - \log_{10} \frac{T_0 \left(\beta M_{cr}^2 + \frac{1}{\gamma} \right)}{P_0 \alpha \beta M_{cr}^2} \quad (3)$$

where

$$\alpha = \frac{\gamma + 1}{\gamma - 1} \quad \beta = \frac{\gamma - 1}{2\gamma}$$

Solving for the critical Mach number (M_{cr}) and utilizing a theoretical Mach number (M_{Dth}) of detonation for infinite tube size and no additives, one can express the fractional maximum Mach number decrement as:

$$\frac{\Delta M}{M}_{\max} = \frac{M_{Dth} - M_{cr}}{M_{Dth}} \quad (4)$$

When the maximum decrement is reached, or exceeded, it is expected that the detonation will quench.

Since water vapor is a very efficient third body, adding small amounts of water vapor to hydrogen-oxygen mixtures should have a pronounced effect on the maximum allowable Mach number decrement, and thus provide a sensitive check on the correctness of Belles' explosion limit criterion. Figure 1 shows the results of typical calculations of the maximum allowable decrement for two hydrogen-oxygen mixtures containing from 0% to 4% (by volume) of added water vapor. The fractional decrements in this figure, and all other decrements given in this paper, are based on an M_{Dth} of 5.28 for the stoichiometric mixture and 5.14 for the 50% H_2 + 50% O_2 mixture.

The feasibility of checking Belles' criterion with explosive mixtures which are not near the composition limits rests on the ability to decrease the detonation Mach number of a specified explosive composition. Specifically, the detonation must be slowed to the critical Mach number given by Eq. (3). Two effects which will result in slowing the detonation have been examined theoretically—these are the effect of a finite sized detonation tube as discussed by Fay⁽⁴⁾, and the effect of a compressible boundary as discussed by Dabora⁽²⁾ and Sommers⁽⁵⁾.

Fay's analysis is based on boundary layer growth within the reaction zone. Since stream lines enter the growing boundary layer, and are concentrated near the wall of the detonation tube, the effect of the boundary layer is to cause the remaining stream lines in the reaction zone to diverge. On this basis, Fay obtains the result that

$$\frac{\Delta V}{V} = \frac{2.1 \delta^*}{d} \quad (5)$$

where δ^* = displacement thickness at C-J surface

d = tube diameter

Dabora developed a solution for the Mach number decrement of a detonation which is exposed to a compressible boundary. The decrement is expressed in terms of the reaction length of the detonation (distance from the shock front to the C-J plane), the explosive channel width, and the density parameter

$$\left(\frac{\rho_e \gamma_e}{\rho_i \gamma_i} \cdot \frac{\gamma_i}{2(\gamma_i + 1)} \right)^{1/2}$$

which gives the relative effectiveness of the inert compressible boundary in confining the detonation. Dabora's analysis allows one to determine the experimental configuration (explosive channel width and inert gas) required to produce a specified Mach number decrement for a particular explosive gas. The model of the detonation-inert boundary interaction used for this analysis is shown in Fig. 2 and a detailed description of the test section used to obtain the desired experimental conditions is contained in Ref. (2).

Two Mach number decrements must be experimentally determined. The decrement due to the effects of finite detonation tube size and of water addition on the detonation velocity is obtained from measurements of detonation velocity in the tube section immediately preceding the test section. The decrement due to the effect of the nitrogen boundary is obtained from streak photographs of the detonations as they pass through the test section. Before making the comparison with Belles' criterion, the two decrements are combined:

$$\frac{\Delta M}{M}_{\text{total}} = \frac{\Delta M}{M}_{\text{tube size, water addition}} + \frac{\Delta M}{M}_{\text{compressible boundary}} \quad (6)$$

II. EXPERIMENTAL PROCEDURE

The procedure and equipment used are essentially those developed by Dabora⁽²⁾ with two exceptions—the addition of a humidifier to the balloon-filling circuit, and the use of a dewpoint measurement system at the entrance of the test section. A schematic of the system used is given in Fig. 3.

Two methods of adding water vapor to the combustible mixture were used for the series of preliminary experiments. The first method, which shall be called the "moisturizer," makes use of a piece of 1 1/2 in. diameter cast iron pipe filled with sponges and provided with appropriate connections at the two ends. Cellulose sponges were cut to fit the interior diameter and were then tightly packed into the pipe. Water was added through a removable pipe plug. The exterior of the moisturizer was heated with a 200 watt infra-red bulb placed approximately 6 in. from the moisturizer, and premixed hydrogen-oxygen was then slowly flowed from the mixing chamber through the moisturizer and into the balloon. Typical fill times for a 0.1 ft³ balloon were on the order of 30 sec. Using room-temperature dry nitrogen gas, this device produced a dewpoint, as measured by an Alnor Dewpointer of 55-58^oF. But since the H₂-O₂ mixing chamber is located outside the Propulsion Laboratory, and the preliminary tests were made in March, the hydrogen-oxygen mixtures admitted to the moisturizer had a temperature of 35-50^oF. Although the hydrogen-oxygen mixtures were heated by contact with the moisturizer, the dewpoint produced by the moisturizer was reduced to 40-50^oF. A drawback of the moisturizer, due to its design, was that the moisture content of the sponges could not be readily determined or controlled.

The second method of adding water vapor consisted of flowing the combustible mixture through a DeVilbiss No. 40 Nebulizer. The Nebulizer was used on all but the first few preliminary experiments. This device is essentially a glass-enclosed atomizer, with the interior of the glass enclosure

serving as a reservoir for the water. Due to the relatively low temperature of the entering gas, it was necessary to preheat the gas prior to its entry into the Nebulizer. The pre-heating was accomplished in a 6 ft long piece of 1/4 in. copper tubing which was wound in a spiral. The exterior of the tubing was heated with a 200 watt infrared bulb placed about 6 in. from the tubing, which produced a temperature rise of 50-60^oF at a flow rate of 0.1 to 0.2 ft³/min. Initial measurements made with the Alnor Dewpointer showed that the Nebulizer plus heat exchanger was capable of producing a dewpoint of 67-71^oF at a room temperature of 81^oF.

The humidity measurements made prior to, and during, the series of preliminary experiments were made with an Alnor Type 7300 DEWPOINTER (Illinois Testing Laboratories, Chicago, Illinois). This instrument is operated by compressing with a hand pump a small sample of the gas in a lighted observation chamber. When the chamber is rapidly vented to atmospheric pressure, the chamber temperature drops, and the presence or absence of condensed vapor (fog) is noted. A trial and error procedure is followed to find the pressure P₀, necessary to cause condensation when the gas is expanded. For an initial temperature T₀ of the pressurized gas and ambient pressure P_a, the gas temperature after expansion, T_{ex}, which will be equivalent to the dewpoint temperature, can be calculated from the adiabatic relation:

$$T_{\text{ex}} = T_0 \left(\frac{P_a}{P_0} \right)^{(\gamma - 1)/\gamma} \quad (7)$$

The Dewpointer gives repeatable, accurate (± 1^oF) results, but the procedure is time consuming, and is not well suited to monitoring the changing dewpoints which occur during post-run purges, and during pre-run charging with the combustible mixture. For these reasons a system consisting of a Honeywell SSP-129A DewProbe and a thermistor temperature sensor was built to allow continuous readout of the dewpoint. The

operation of the DewProbe is based on two unique characteristics of lithium chloride—it is hygroscopic, and at a relative humidity of 11% or greater, lithium chloride will absorb enough water to become electrically conductive. The DewProbe humidity sensing element consists of a lithium chloride impregnated cloth sleeve which is wound with a two-wire element and is slipped over a metal tube, or bobbin. The two wires are wound next to each other, but are not connected, so that an electric potential placed on the two wires will result in a current flow only when the lithium chloride is conductive. The electric current flow heats the cloth sleeve and metal bobbin until the relative humidity of the moist atmosphere is 11% at that temperature, at which point the lithium chloride becomes nonconductive. The DewProbe element thus maintains itself at the temperature which corresponds to a relative humidity of 11%. Measurement of the bobbin cavity temperature gives the temperature for which the relative humidity is 11%, from which the dewpoint of the moist atmosphere can be determined.

The cavity temperature readout was accomplished by connecting a Fenwell 6A45JI thermistor (selected for its high temperature sensitivity) in series with a 1.34 volt mercury battery power supply and a 0-100 μ amp Simpson Model 1329 meter as shown in Fig. 4. Temperature readout is made in terms of μ amps of current through the variable resistance of the thermistor, from which the temperature of the thermistor and the DewProbe cavity can be obtained. The thermistor-meter-battery system was calibrated against a mercury thermometer (WOODCO M-1100) and against copper-constantin thermocouples and the results are shown in the Appendix, Fig. a. Since the maximum difference between the two calibrations is 1.5^oF, the accuracy of the resulting temperature vs. current calibration is estimated to be \pm 0.8^oF. The cavity temperature readout is converted to dewpoint by

using a Honeywell supplied cavity temperature vs. dewpoint calibration shown in Appendix Fig. b. Accuracy of the DewProbe in the range of interest is stated by Honeywell to be $\pm 0.25^{\circ}\text{F}$ in dewpoint, so the resulting accuracy in dewpoint is taken to be $\pm 1.0^{\circ}\text{F}$.

The mercury battery power supply (two Mallory RM-4RT in parallel) has a very flat voltage vs. time characteristic, but continuing checks on the condition of the batteries were made by switching a known, fixed resistor into the circuit in place of the thermistor—any deviation from the current reading ($65\ \mu\text{amps}$) taken at the time of the original calibration would indicate a change in battery voltage. Since no change in this reading occurred during these experiments, the original calibration was assumed to remain valid. Figure 5 obtained from Appendix Fig. a-c gives the conversion from the meter reading to volumetric concentration of water vapor.

Operationally, the DewProbe proved to be superior to the Alnor Dewpointer due to the ease with which the dewpoint of the system could be monitored. However, it had two disadvantages, the first of which is poor response to large, fast changes in dewpoint. It is believed that this was due to the absorption of a large amount of water vapor by the DewProbe bobbin, which caused a virtual short circuit of the heating element. This overloaded the DewProbe transformer, and caused a reduced potential (0.5 volts vs. a nominal 28.0 volts) across the heating element, which resulted in a substantial delay before the DewProbe bobbin reached an equilibrium temperature and evaporated the excess moisture. To avoid this difficulty, the system was purged to an intermediate dewpoint (about 40°F) after each run, and then slowly brought up to the equilibrium dewpoint with moist $\text{H}_2 + \text{O}_2$ mixture prior to the next run.

The other disadvantage of the DewProbe is that it cannot measure very low dewpoints—for an ambient temperature in the 78-82^oF range, the lowest dewpoint which can be measured is in the 19-23^oF range. This limitation affected only those runs made with a "dry" mixture, i. e., once the minimum dewpoint reading was obtained, it could only be assumed that continued flowing with a dry mixture would lower the dewpoint of the system.

Until the DewProbe system was installed, it was not realized that the detonation tube and the plumbing used to charge the system with moist H₂ + O₂ mixture were absorbing water. This absorption of water was first noted when it was found that approximately 0.5 ft³ of moist mixture were required to produce an indication of increased dewpoint at the DewProbe if the system had been purged out after the preceding run. (The DewProbe itself required 0.1 or at most 0.2 ft³ of gas to reach an equilibrium reading.) It was this situation which first resulted in doubt as to the dewpoint actually obtained during the preliminary tests, since these tests were made by flowing only 0.2 ft³ of moist H₂ + O₂ through the system after it had been purged for approximately 20 minutes with dry N₂.

Run Procedure: (Refer to Fig. 3)

1. Connect DewProbe to the detonation tube, by removing ionization probe No. 3, inserting an adapter in its place, and connecting the DewProbe tubing.
2. Purge the system with dry N₂, by opening V-17, to a dewpoint of 30-40^oF. Progress of purge is monitored with an EICO Model 221 VTVM connected to the DewProbe thermistor leads.
3. Install balloon at the adaptor downstream of valve V-8.
4. Close V-17, V-14, and V-9, and evacuate this part of the system.
5. Open V-14. Then open V-5 until a pressure of 5 psig is indicated on pressure gage P-1. This operation fills the balloon with moist H₂ + O₂ mixture.

6. Close V-14 and open V-9 one turn to flow the mixture through the detonation tube and DewProbe. Monitor system dewpoint with the EICO VTVM.
7. Repeat step 6 until a steady dewpoint reading is obtained.
8. Refill the balloon with moist mixture, and open V-9 three turns (runs are made with V-9 opened three turns). Monitor system humidity with the Simpson microammeter. If any changes occur during this balloonful, repeat this step until a stable reading is obtained. Record the microammeter reading obtained before the balloon is empty.
9. Remove the DewProbe tubing, adapter, and insert ion probe No. 3 into the detonation tube, while the balloon is maintaining a positive pressure on the system.
10. Load the rotating drum camera with film (note, this step is usually accomplished during the pre-run purge).
11. Insert the nitrocellulose film, on its holder, into the test section.
12. Refill the balloon with moist $H_2 + O_2$ mixture.
13. Close V-8 and V-14, and evacuate the closed-off part of the system. This is a safety feature designed to reduce the possibility of the detonation propagating back into the Nebulizer/moisturizer and the mixing chamber.
14. Open V-9 three turns, maintaining an equal pressure on both sides of the nitrocellulose film by opening and closing V-1 as required.
15. Bring the rotating drum camera up to full speed.
16. When the balloon is almost empty, initiate the detonation.
17. Record data:
 - 1) τ_{13} —detonation time from time-interval counter.
 - 2) Manometer (P-2) reading.
 - 3) Temperature at level of test section and floor.

III. EXPERIMENTAL RESULTS

A. Preliminary Experiments

A series of preliminary experiments was made with 50% H₂ + 50% O₂ (by volume) mixtures in order to determine if the addition of water vapor did have an effect on the characteristics of detonation wave propagation. The 50% H₂ mixture was selected because it emphasizes the effect of water addition on the effective third body concentration given by Eq. (2). It was apparent from analysis of the rotating drum camera photographs that the addition of small amounts of water vapor did have an effect on the Mach number decrement due to a compressible boundary. The Mach number decrements obtained from these experiments are summarized on Fig. 6.

Dewpoint measurements made with the Alnor DEWPOINTER prior to and during the preliminary experiments showed the mixtures were approximately 25% saturated, corresponding to approximately 1% by volume of water vapor.

As a result of the preliminary experiments, the Honeywell DewProbe dewpoint measurement system was installed, and a more extensive series of experiments on stoichiometric hydrogen-oxygen mixtures was made.

B. Detonation Velocity Measurements

In the absence of appropriate detonation velocity data for hydrogen-oxygen mixtures with small amounts of water added, a series of tests were run on the 50% H₂ + 50% O₂ and 66 2/3% H₂ + 33 1/3% O₂ mixtures. The experimental data are presented in Fig. 7 along with the theoretical velocity predictions from Gordon⁽⁶⁾ for the stoichiometric H₂-O₂ mixtures. The Mach number decrement due to finite tube size and water addition is calculated from the experimental data for use in Eq. (6).

Scatter in the velocity data is attributed principally to small variations in the hydrogen-oxygen ratio due to the mixture preparation technique. The velocity error represents approximately $\pm 0.5\%$ variation in the percentage of hydrogen in the mixtures. For this reason, the curve for the stoichiometric mixture was drawn to follow the trend of the data from a particular filling of the mixing chamber, and was then shifted so as to represent the average of the data. It should also be noted that the water content of the data plotted at $0.0\% \text{ H}_2\text{O}$ could be as high as $0.3\% \text{ H}_2\text{O}$ since the minimum measurable dewpoint corresponded to 0.3% . However, the moisture content was considered to be closer to 0.0% , since purging with commercially dry N_2 was continued for 20 minutes after the minimum readable dewpoint was obtained, and the detonation tube was then charged with dry $\text{H}_2\text{-O}_2$ mixture. The curve for the $50\% \text{ H}_2 + 50\% \text{ O}_2$ mixtures was drawn as a straight line between the average velocities of the two groups of data shown as no experiments were performed at the intermediate points.

C. Compressible Boundary Effects

Streak photographs were obtained with a rotating drum camera for several test section channel widths. These photographs give a distance vs. time trace of the detonation wave as it travels through the test section, so that the change of slope of the trace will give the velocity decrement, $\Delta V/V$, suffered by the detonation when it is exposed to the compressible (nitrogen) boundary. Since Belles' criterion is based on the calculation of a critical Mach number, it is necessary to assess the effect of water addition on conversion of the velocity decrement data to a Mach number decrement. The experimental data gives $\Delta V_w/V_w$ from which it is desired to obtain $\Delta M_w/M_{Dth}$. Then

$$\frac{\Delta M_w}{M_{Dth}} = \frac{\Delta M_w}{M_w} \cdot \frac{M_w}{M_{Dth}} = \frac{\Delta M_w}{M_w} \cdot \frac{V_w}{a_w} \cdot \frac{a_{th}}{V_{Dth}} \quad (8)$$

where $\Delta V_w/V_w \equiv \Delta M_w/M_w$ and the ratio V_w/V_{Dth} is evaluated from the experimental velocity data by considering only the effect of water vapor, i. e., by excluding the effect of finite tube size. Evaluated at a 2% (by volume) concentration of water vapor in stoichiometric H_2-O_2 , the ratio $V_w/V_{Dth} \cdot a_{th}/a_w = (.984)(1.006) = .990$ which may be considered unity. To this approximation,

$$\frac{\Delta M_w}{M_{Dth}} = \frac{\Delta V_w}{V_w} \quad (9)$$

A summary of the data obtained on the Mach number decrements due to the effect of the compressible nitrogen boundary is presented in Fig. 6 and 8, and on Table 1. Dabora's equation for $\Delta M/M$ (Eq. (2.27) of Ref. 2) was utilized to draw the curves on Fig. 6 and 8 by determining the reaction lengths \bar{x} required to produce agreement with the experimental data. These lengths are shown in Table II.

Examination of Fig. 6 and 8 reveals three significant features—(a) the decrease in Mach number decrement for a given channel width when water vapor is added to the explosive mixture, (b) the agreement between the predicted and experimental level of the maximum Mach number decrement, and (c) the indicated decrease in Mach number decrement for mixtures with and without water added as the quenching limit is approached.

The significant decrease in Mach number decrement when water vapor is added is most plausibly explained by assuming that the reaction length (the distance from the shock wave to the Chapman-Jouguet plane) is decreased by the addition of small amounts of water vapor. The Mach number decrement data are fitted to the theoretical prediction of $(\Delta M/M)_{comp}$ of Dabora⁽²⁾ when the reaction lengths in Table 2 are used.

TABLE 1. SUMMARY OF DATA

$\frac{\%H_2}{\text{in } H_2-O_2}$	b inch	No. of runs	$\% H_2O$ by Vol.	* V ft/sec	$\Delta M/M$
50	.5	4	est. < .3	7370 + 160 - 168	.062 + .023 - .017
	.5	6	est. 1.0 ± .5	7416 + 299 - 139	.044 + .020 - .023
	.4	4	est. < .3	7476 + 71 - 27	.077 + .026 - .033
	.4	6	est. 1.0 ± .5	7449 + 98 - 37	.044 + .011 - .010
	.35	3	est. < .3	7339 + 42 - 36	.068 + .013 - .012
	.35	4	est. 1.0 ± .5	7476 + 210 - 234	quench
	.3	3	est. < .3	7407 + 16 - 16	quench
	66 2/3	.4	4	1.88 + .15 - .30	9068 + 48 - 47
.35		4	2.00 + .15 - .30	9052 + 136 - 70	.024 + .016 - .011
.3		4	1.74 + .57 - .34	9076 + 186 - 71	.045 + .008 - .008
.25		4	1.85 + .20 - .15	9044 + 48 - 31	.045 + .022 - .018
.20		5	1.94 + .24 - .26	9037 + 15 - 16	.020 + .006 - .009
.15		3	2.00 + .30 - .42	8997 + 24 - 38	quench

*Measured by ionization probes

TABLE 2. REACTION LENGTH

<u>Mixture</u>	<u>Reaction Length</u> inches
(66 2/3% H ₂ + 33 1/3% O ₂), 2% water vapor added	.058
66 2/3% H ₂ + 33 1/3% O ₂ , dry	.128
(50% H ₂ + 50% O ₂), 1% water vapor added	.108
50% H ₂ + 50% O ₂ , dry	.160

The comparison between experimental data and Belles' predicted explosion limit was hampered by the existence of an unsteady phenomenon (spin) which appear near the limits of detonability and by practical considerations which limit the increments in channel width to 0.05 inches. Therefore, the exact value of the maximum Mach number decrement could not be experimentally determined. Of the two, the unsteady behavior of the detonation is more fundamental obstacle to an exact determination of the quenching limit. The unsteadiness which is observed near the limit is apparently the spin phenomenon described by a number of investigators, including Dove and Wagner⁽⁸⁾. It is interesting to note that the onset of pronounced unsteadiness results in a decrease in the measured velocity decrement, i. e., the points for $b = .3$ in. with H₂O, $b = .35$ in. without H₂O on Fig. 6 and for $b = .2$ in. with and without H₂O on Fig. 8. The reduction in velocity decrement is probably due to the way in which the decrements were measured—that is, the average slope of the peaks of the detonation trace were used. The decrement obtained in this way may not be representative of the true time average of the propagation velocity since the shape of the position vs. time trace is quite complex and not at all regular. Nevertheless, the peaks of the waves do appear to travel at a "steady" average velocity, and the detonation shows no signs of definitely quenching within the observable length of the test section.

From Fig. 6 and 8, it is apparent that the extrapolated experimental Mach number decrement curves intersect Belles' explosion limit in the region between the channel width which experimentally results in pronounced unsteadiness (spin), and the channel width which produces definite quenching of the detonation wave within the test section. The $(\Delta M/M)$ lines labeled "Belles' Explosion Limit" on Fig. 6 and 8 represent the theoretical maximum decrement which the compressible boundary alone can induce before quenching occurs. They are obtained by subtracting the experimentally determined values of the Mach number decrement due to finite tube size and water vapor addition from the appropriate values in Fig. 1. The observed agreement between the predicted and experimental level of the maximum Mach number decrement supports Belles' formulation of the limits of detonability. Specifically, the strong influence of water vapor on the second explosion limit, through its effect on the effective third body concentration, is seen to have a similar effect on the quenching limit of detonative combustion.

IV. DISCUSSION

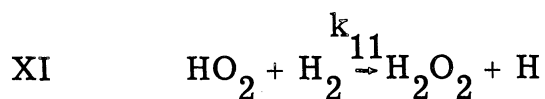
Belles' formulation of the limits of detonability utilizes two chemical-kinetic assumptions which are not obviously valid: (a) that the concentration of H_2 , O_2 , and H_2O do not change in the induction zone, and (b) that the HO_2 radicals produced by reaction VI are inert in the induction zone.

The constancy of (H_2) and (O_2) can be inferred from the extremely small concentrations of H, OH, and O produced in the induction zone, and from the fact that the dissociation of H_2 and O_2 in the induction zone is negligible, as shown by Nicholls⁽⁹⁾. The approximation (H_2O) = const. in the induction zone rests on the fact that very little H_2O is produced initially by the H_2 , O_2 reaction, and so in the induction zone only the dissociation of H_2O need be considered. For the dissociation of H_2O , Bauer, Schott and Duff⁽¹⁰⁾ prefer either of the two decomposition reactions



as a path to dissociation in the temperature range of 2400° - 3200° K. However even though these reactions have lower activation energies (~ 45 Kcal/mole) than that of the direct dissociation (~ 70 Kcal/mole) the temperature behind the shock in our case is low enough to preclude appreciable amount of dissociation.

Assumption (b) is more difficult to rationalize. Specifically, the gas phase reaction of HO_2 has been stated by Lewis and von Elbe⁽³⁾ to be:



In addition, Miyama, and Takeyama⁽¹¹⁾ used reaction XI in an analysis of the reactions in shocked argon, hydrogen and oxygen mixtures, and found an activation energy of 14.8 ± 2.2 Kcal/mole, which is of the same order of magnitude as the controlling reaction, reaction II. From this point of view, the approximation that HO_2 is an inert molecule in the induction is not particularly good. Furthermore, if reaction XI for HO_2 is included in the reaction scheme, and the time rate-of-change of active radicals is calculated, it is found that there is no simple requirement, like $2k_2 = k_6(X)$, for which the time rate-of-change of active radicals is zero. However, Brokaw⁽¹²⁾ has included reaction XI in an analysis of induction times, and concludes that if the "explosion limit" condition $2k_2 = k_6(X)$ is invoked, the induction time increases by approximately two orders of magnitude as the lean limit of detonability is approached. This means that the time rate-of-change of active radicals becomes very small, but not zero, when the condition $2k_2 = k_6(X)$ is invoked.

In an experimental situation, nonsteady phenomena become pronounced as the limit of detonability is approached and the determination of the exact limit is difficult and therefore it is not possible to distinguish between Belles' and Brokaw's statements on the limit of detonability. Hence, within experimental limits, the assumption that HO_2 is an inert molecule in the induction zone results in a correct limit of detonability.

Although the effect of water vapor on the induction zone can be theoretically determined, its effect on the remainder of the reaction zone is still not defined. At present there is no theoretical justification for postulating that the addition of water vapor shortens the reaction length in hydrogen-oxygen detonations. However, the experimental work of Kistiakowsky and Kydd⁽⁷⁾ seems to lend support to this conclusion. These authors studied the density variation with time behind shocked mixtures

of xenon, hydrogen, oxygen and various additives including water vapor, and concluded in part that water vapor has no retarding effect on the reaction. However, the part of their data which is pertinent to this work was re-examined and their data for mixtures containing $2\text{H}_2 + \text{O}_2 + 1/2 \text{Xe}$, $2\text{H}_2 + \text{O}_2 + 1/2 \text{Xe} + 1/4 \text{H}_2\text{O}$, and $2\text{H}_2 + \text{O}_2 + 1/2 \text{Xe} + 1/2 \text{H}_2\text{O}$ are plotted in Fig. 9. It is seen that adding water vapor results in a faster rise to a higher peak density and a faster decay to the equilibrium density, (the C-J density). Although the data for the mixture containing $1/2 \text{H}_2\text{O}$ shows a slight increase in reaction time compared to the mixture containing $1/4 \text{H}_2\text{O}$, it is apparent that either of these mixtures has a reaction length lower than that of the dry mixture. Thus these data can be considered to confirm our findings regarding the reaction length.

V. CONCLUSIONS

It has been experimentally verified that, for 50% H₂ + 50% O₂ and 66 2/3% H₂ + 33 1/3% O₂ mixtures, the addition of water vapor increases the minimum required Mach number of propagation. This finding is in agreement with the explosion limit criterion given by Belles. Specifically, the high efficiency of water vapor as a third body in the chain breaking reaction, has been verified for detonative combustion. In addition, it was found that the addition of water vapor to both the 50% H₂ and 66 2/3% H₂ mixtures acted to reduce the Mach number decrement due to the compressible boundary when the same channel width and boundary gas are used. This reduction in Mach number decrement is explained by postulating a reduction in reaction length. The experimental work of Kistiakowsky and Kydd was found to give further support to this conclusion.

REFERENCES

1. Belles, F. E. , "Detonability and Chemical Kinetics, Prediction of Limits of Detonability of Hydrogen," Seventh Symposium (International) on Combustion, 745-751, Butterworths, London, 1959.
2. Dabora, E. K. , The Influence of a Compressible Boundary on the Propagation of Gaseous Detonations, Ph. D. Thesis, The University of Michigan, December 1963. See also Proceedings of Tenth Symposium (International) on Combustion, to be published.
3. Lewis, B. and von Elbe, G. , Combustion, Flames, and Explosions of Gases, 2nd ed. , Chapt. 1, Academic Press, New York, 1961.
4. Fay, J. A. , "Two-Dimensional Gaseous Detonations: Velocity Deficit," The Phys. of Fluids, Vol. 2, No. 3, 283-289, May-June 1959.
5. Sommers, W. P. The Interaction of a Detonation Wave with an Inert Boundary, IP-501, The University of Michigan Industry Program of the College of Engineering, Ann Arbor, March 1961.
6. Gordon, S. , private communication.
7. Kistiakowsky, G. B. and Kydd, P. H. , "Gaseous Detonations. IX. A Study of the Reaction Zone by Gas Density Measurements," J. Chem. Phys. , 25, 824-835, 1956.
8. Dove, J. E. and Wagner, H. Gg. , "A Photographic Investigation of the Mechanism of Spinning Detonation," Eighth Symposium (International) on Combustion, 589-600, Williams and Wilkins, Baltimore (1962).
9. Nicholls, J. A. , Stabilization of Gaseous Detonation Waves with Emphasis on the Ignition Delay Zone, Report No. IP-421, Industry Program of the College of Engineering, The University of Michigan (1960).
10. Bauer, S. H. , Schott, G. L. , and Duff, R. E. , "Kinetic Studies of Hydroxyl Radicals in Shock Waves. I. The Decomposition of Water Between 2400⁰ and 3200⁰K," J. Chem. Phys. , 28, No. 6, 1089-1096 (1958).
11. Miyama, H. and Takeyama, T. , "Kinetics of Hydrogen-Oxygen in Shock Waves," J. Chem. Phys., 41, No. 8, 2287-2290 (1964).
12. Brokaw, R. S. , Analytic Solutions to the Ignition Kinetics of the Hydrogen-Oxygen Reaction, NASA TMX 52003 (1964). See also Tenth Symposium (International) on Combustion, to be published.

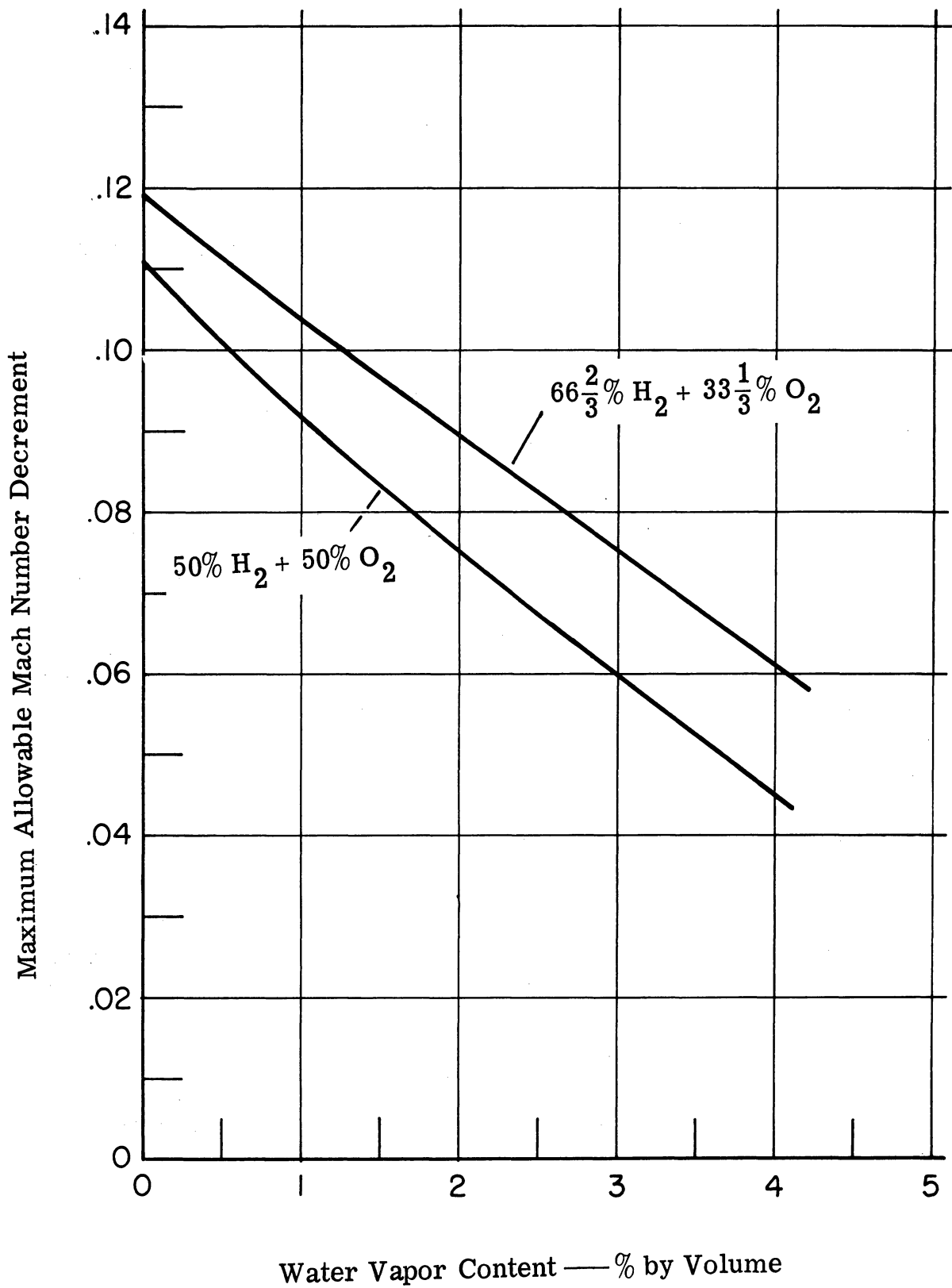


Figure 1. Maximum Allowable Mach Number Decrement as a Function of Water Vapor Content

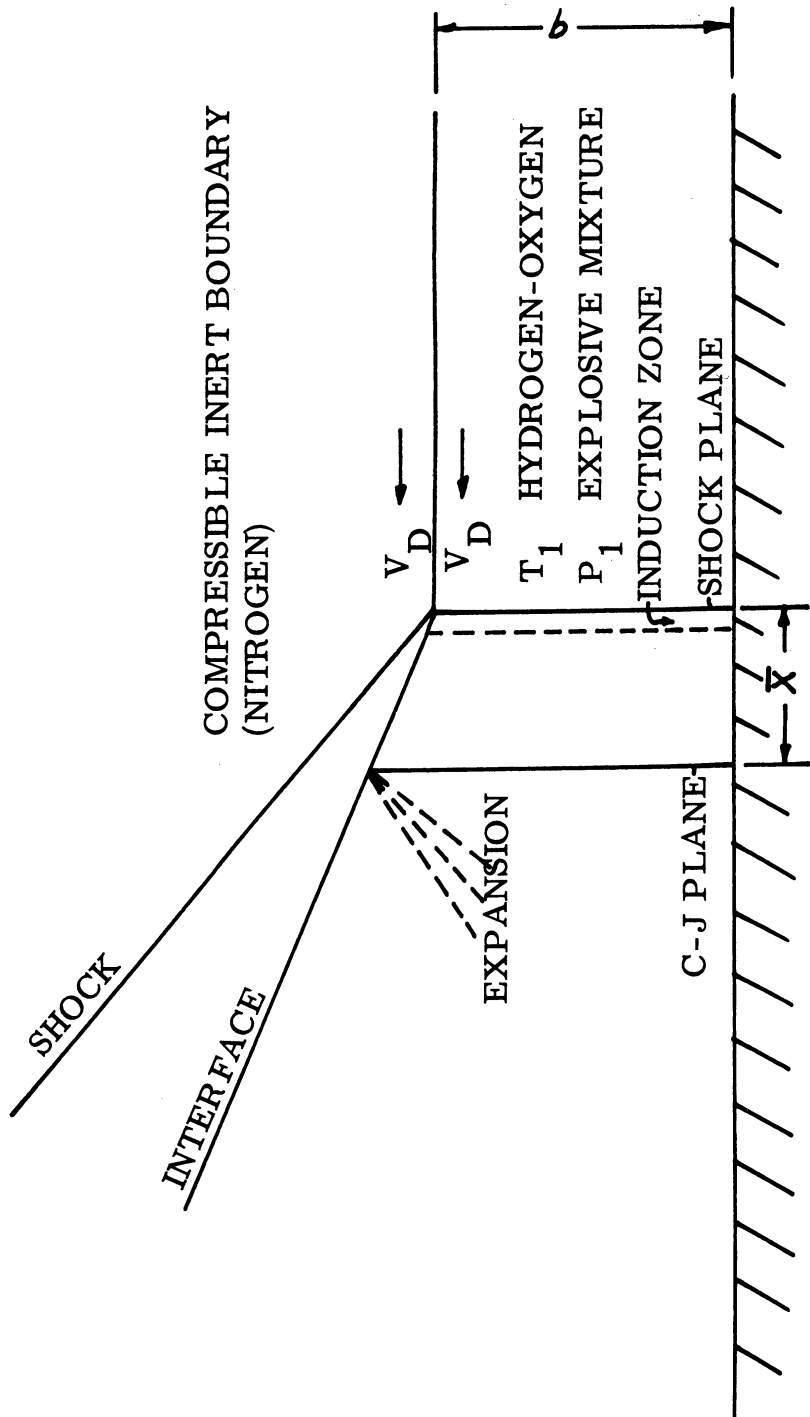


Figure 2. Model for the Interaction of a Detonation With a Compressible Inert Boundary

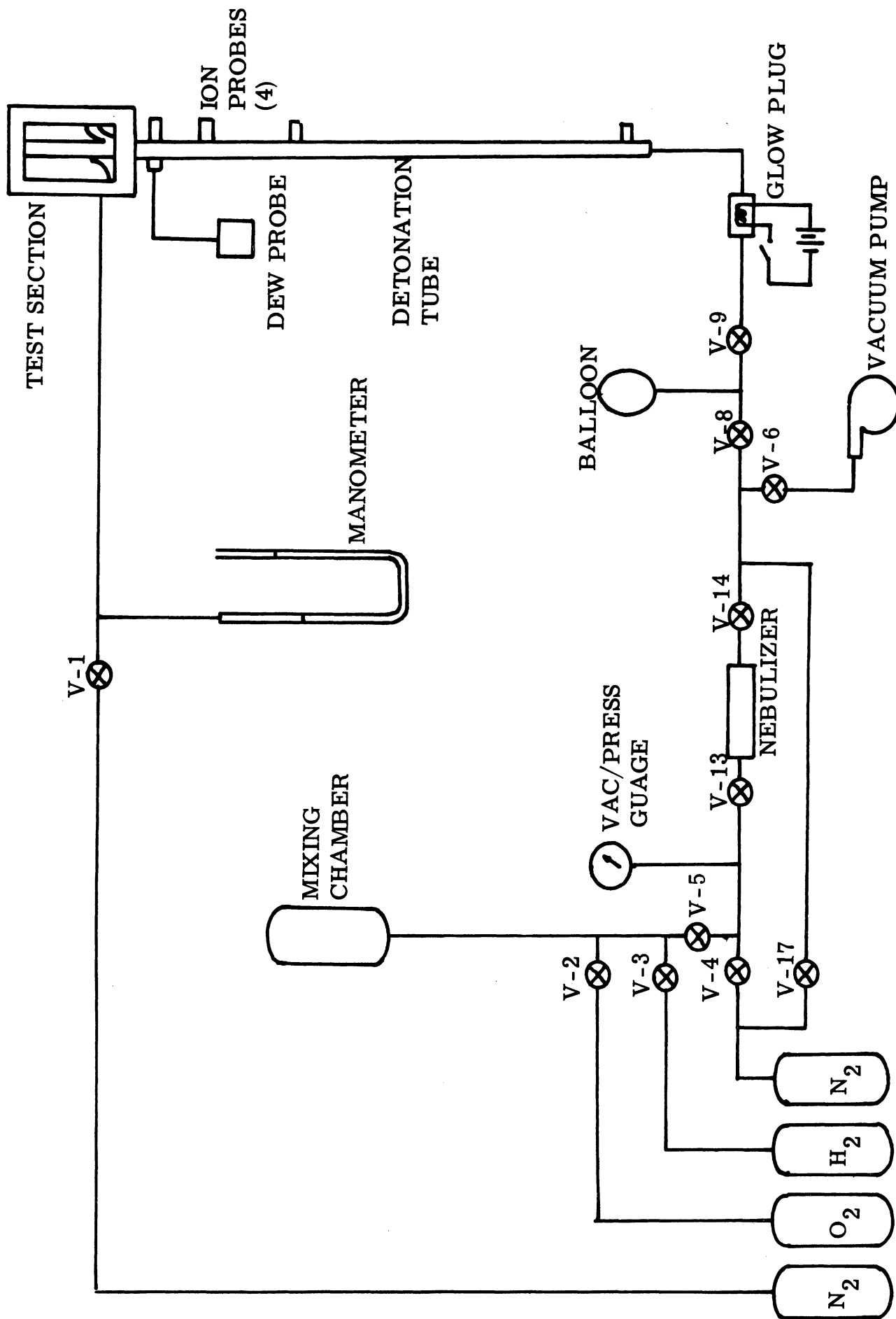


Figure 3. Schematic of Mixing and Charging System

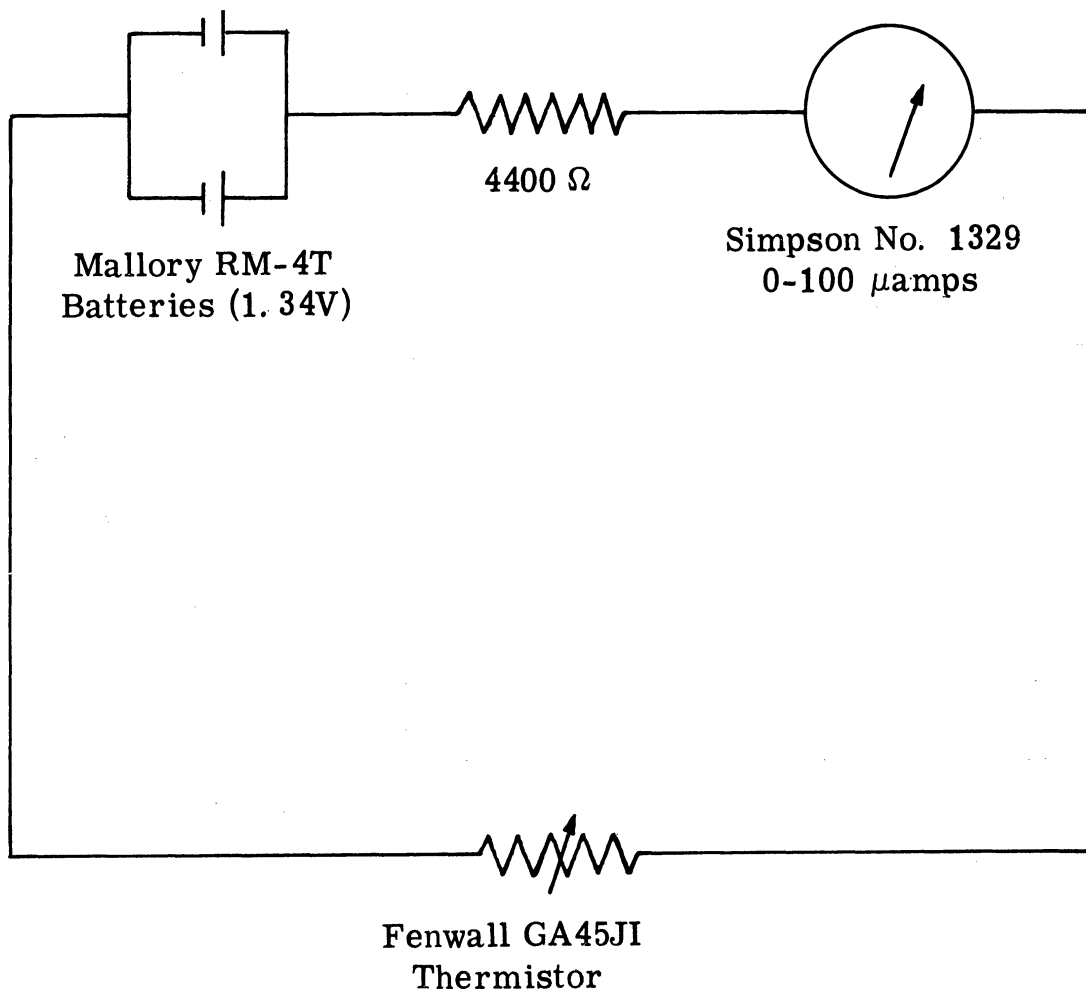


Figure 4. Circuit Diagram for DewProbe Cavity Temperature Measurement

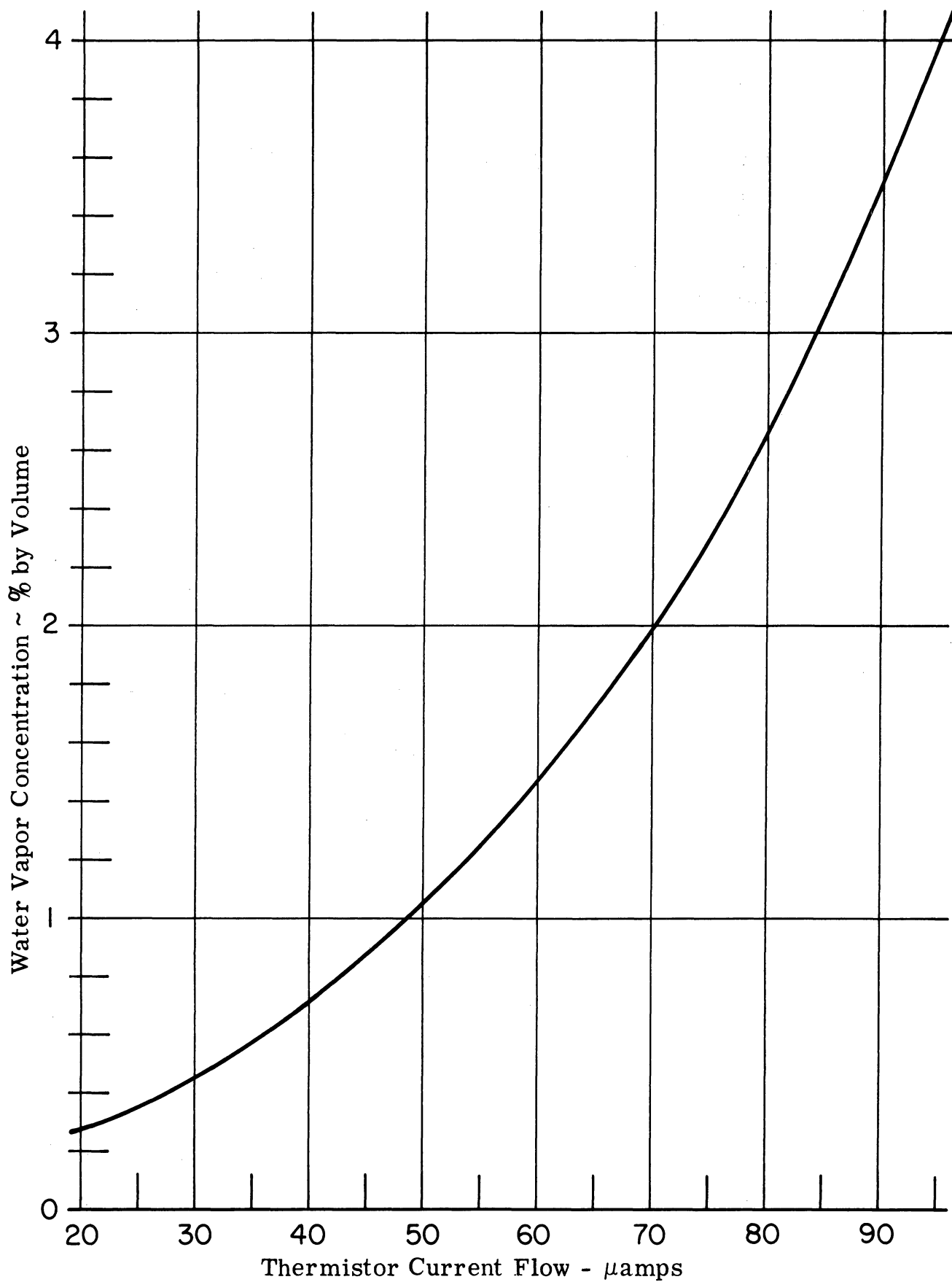


Figure 5. Curve for Use in Determining Water Vapor Content of Explosive Mixture from Thermistor Current Flow

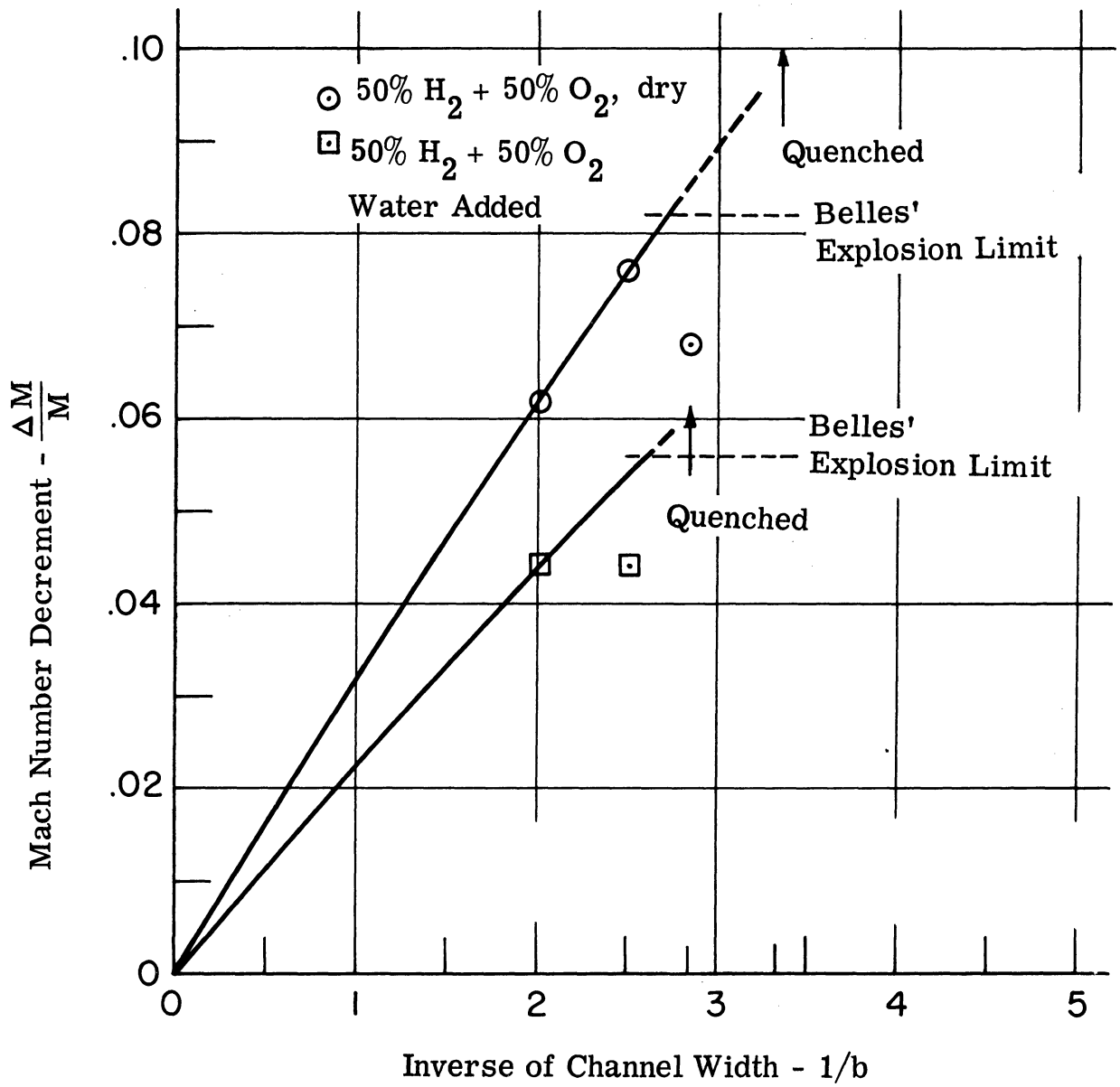


Figure 6. Experimental Mach Number Decrement Due to the Compressible Boundary as a Function of Channel Width . 50% H₂ + 50% O₂ Mixture.

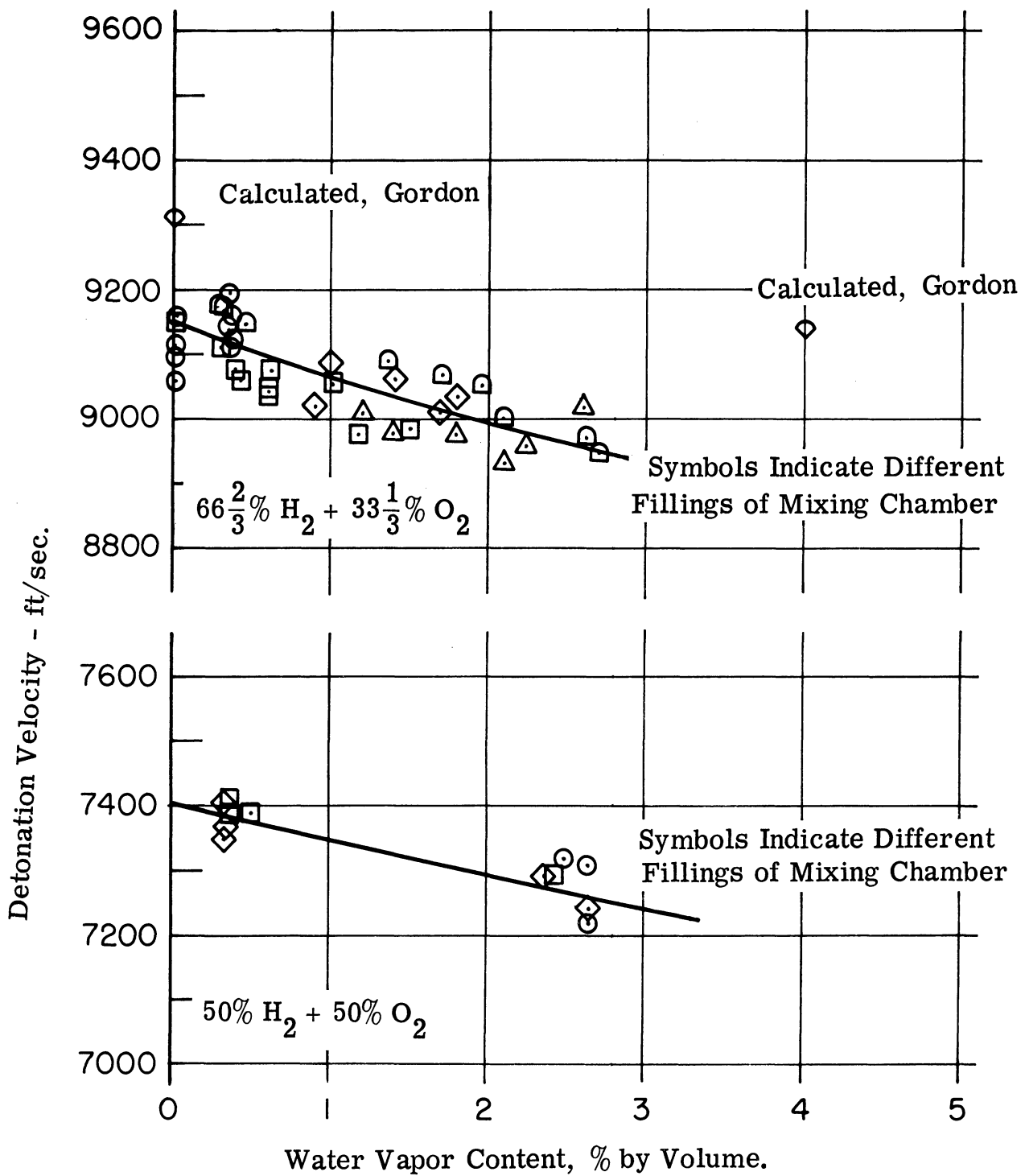


Figure 7. Detonation Velocity of $50\% \text{H}_2 + 50\% \text{O}_2$ and $66\frac{2}{3}\% \text{H}_2 + 33\frac{1}{3}\% \text{O}_2$ Mixtures as a Function of Water Vapor Content

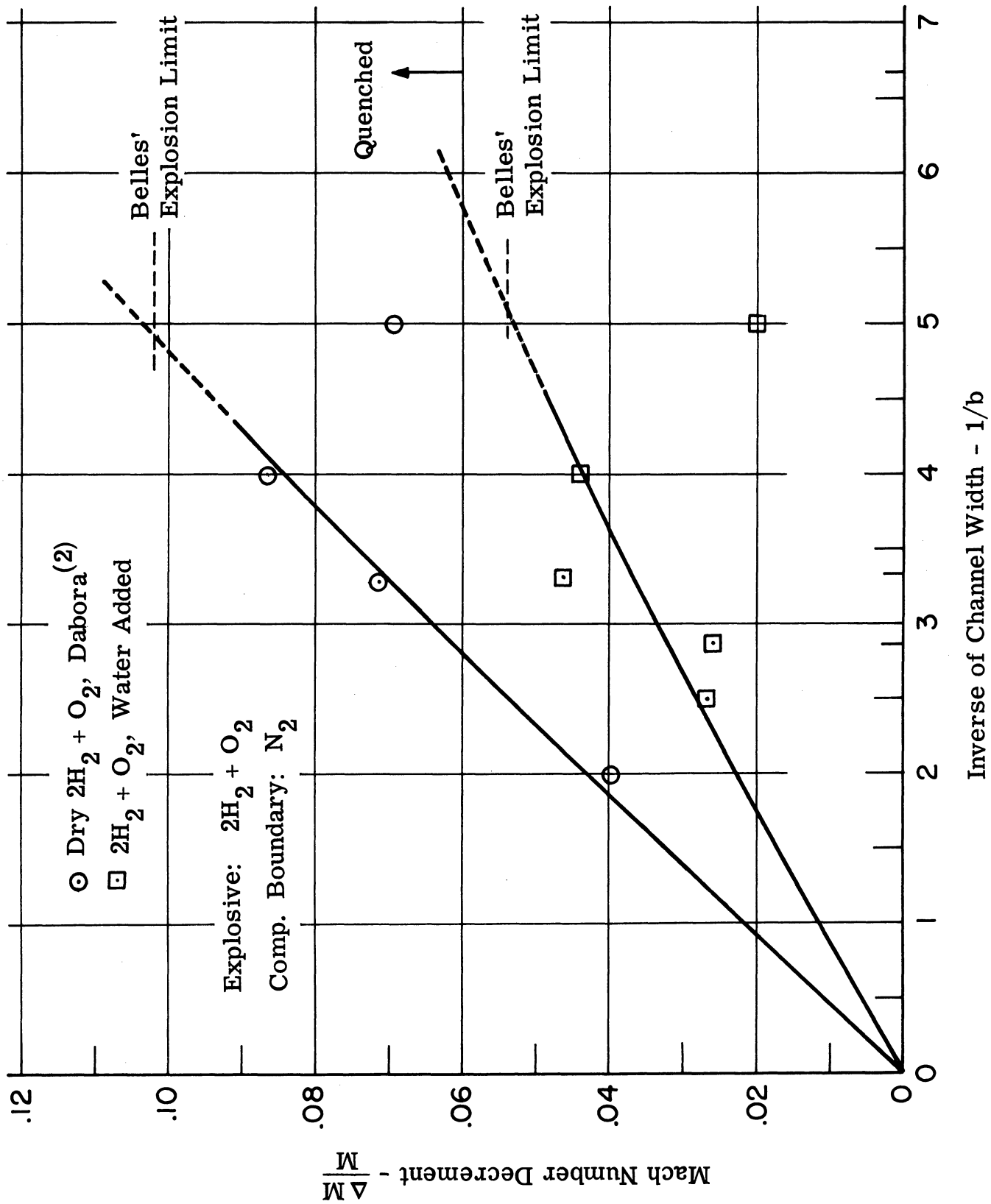


Figure 8. Experimental Mach Number Decrement Due to the Compressible Boundary as a Function of Channel Width. 66 2/3% H_2 + 33 1/3% O_2 Mixture.

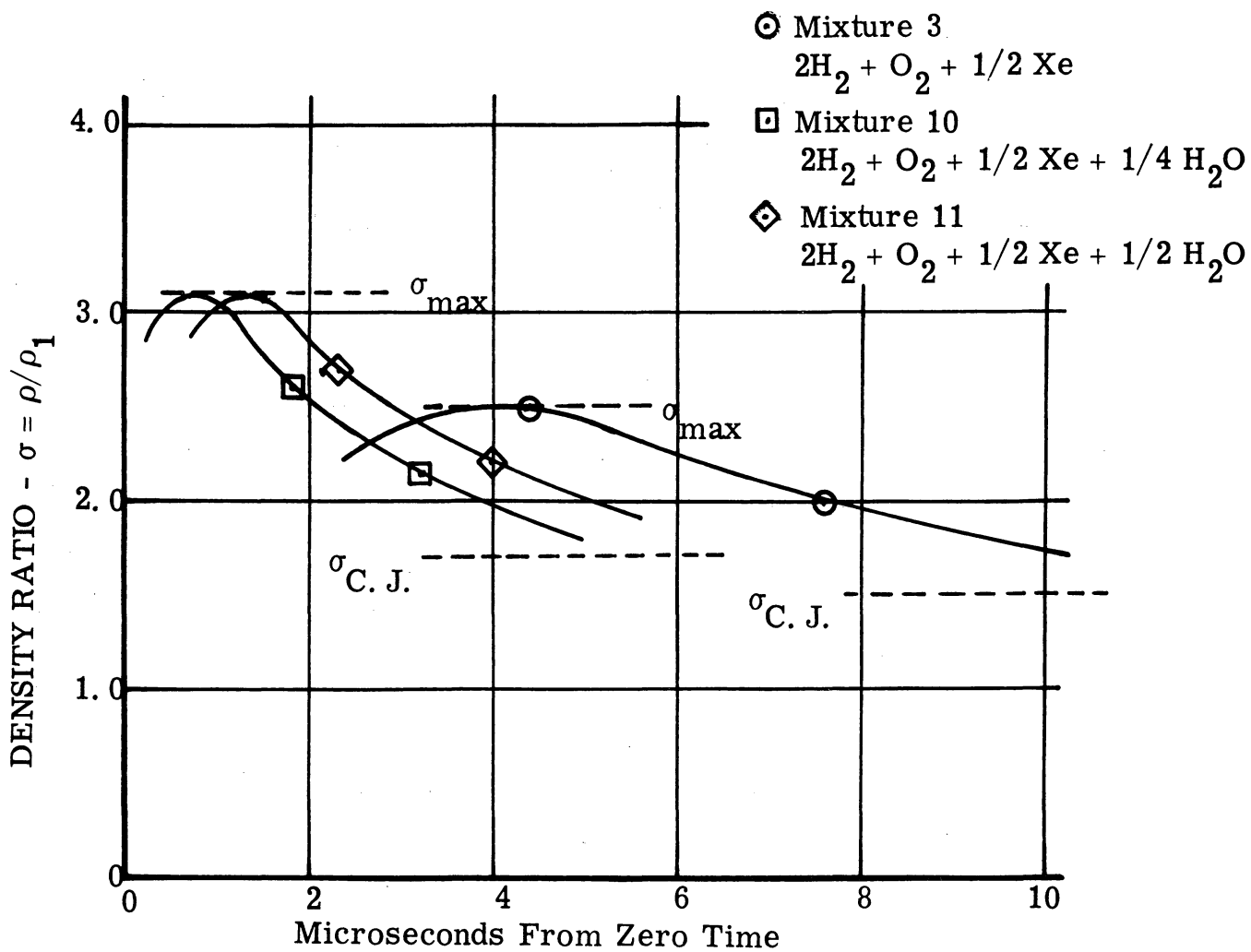


Figure 9. Density Changes in a Hydrogen-Oxygen Detonation as a Function of Time. Data from Kistiakowsky and Kydd⁽⁷⁾.

Appendix I

CALIBRATION CURVES FOR DEWPROBE/THERMISTOR DEWPOINT MEASUREMENT SYSTEM

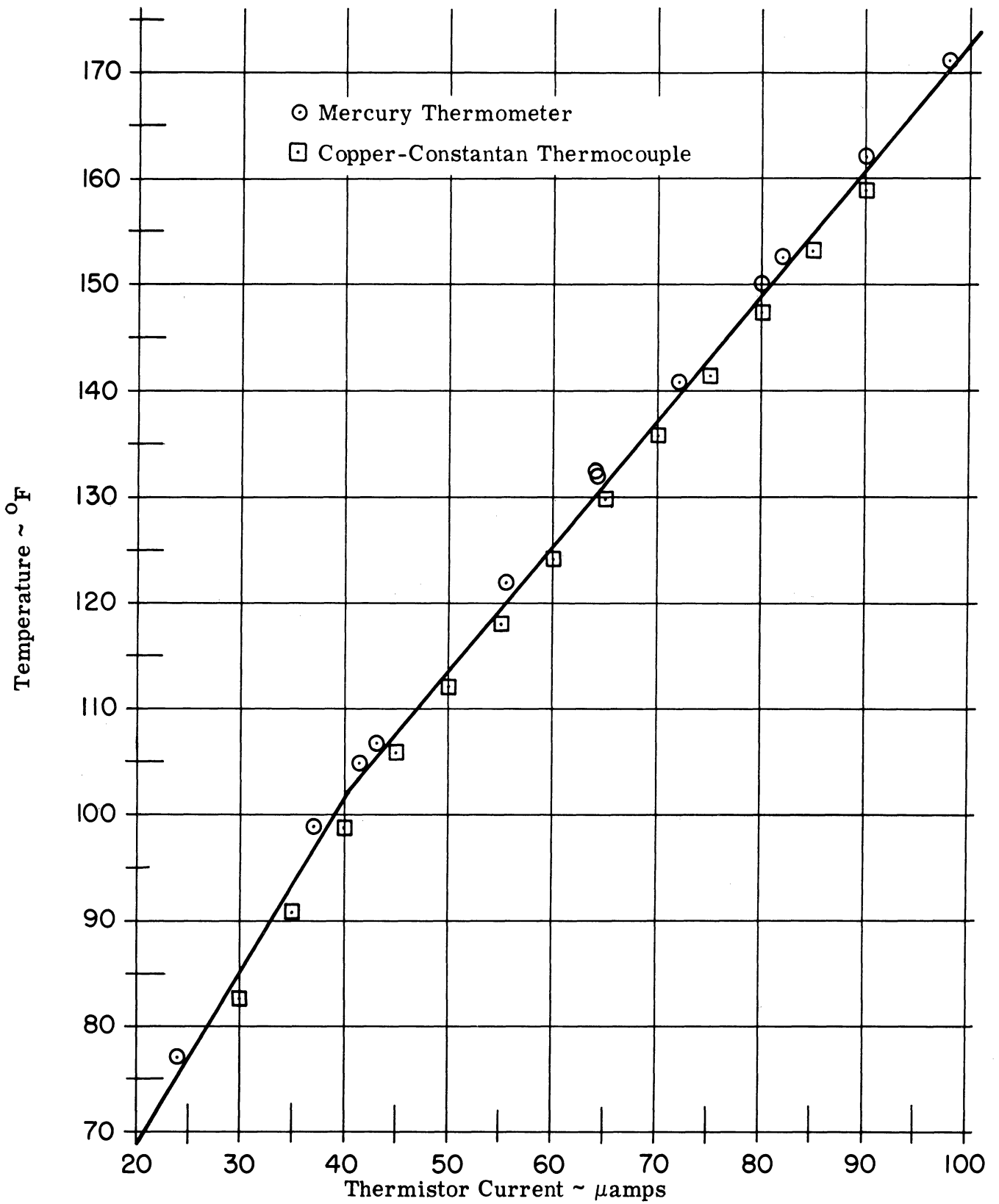


Figure a - Thermistor Calibration
 Temperature vs. Current Through Thermistor

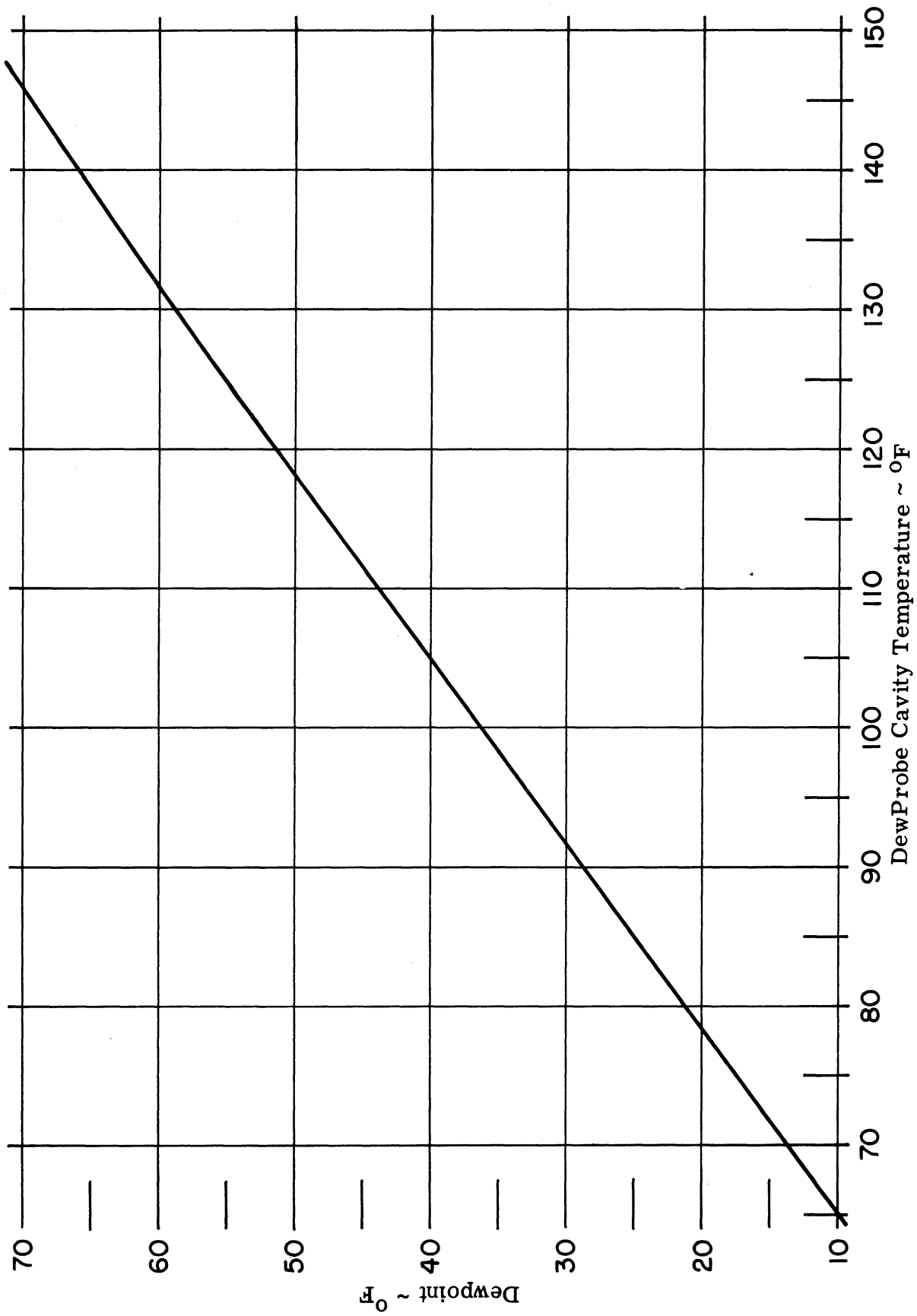


Figure b - Dewpoint vs. DewProbe Cavity Temperature
 (Data from Honeywell Special Sensor Products Div.)

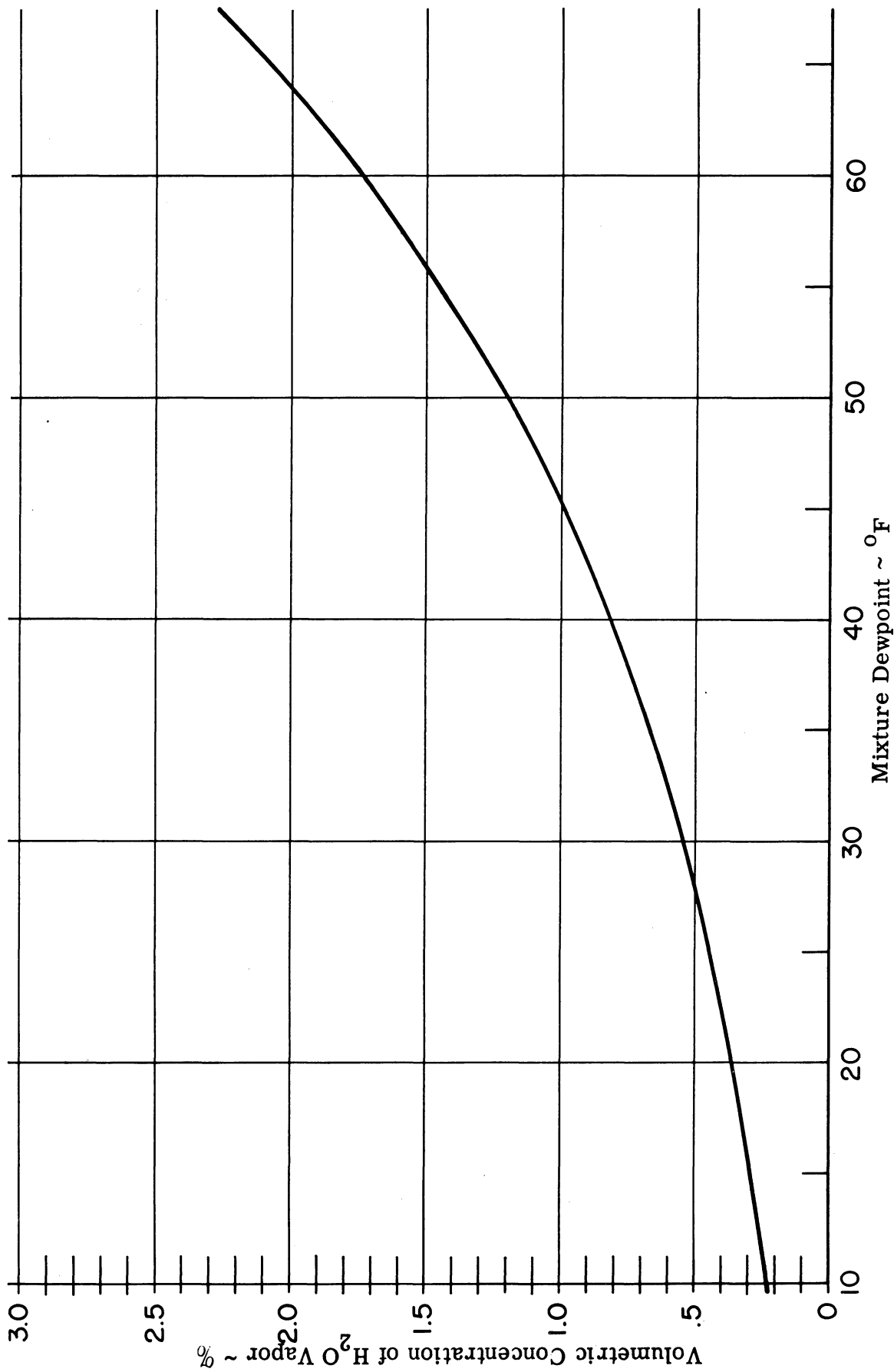


Figure c - Volumetric Concentration of H₂O Vapor vs. Mixture Dewpoint
 (Data from Handbook of Chemistry and Physics, 36th Edition)

15.0 psia Ambient Pressure

UNIVERSITY OF MICHIGAN



3 9015 03023 8292